Processes Governing the Evolution of Moist Static Energy in Developing and Non-developing African Easterly Waves

Kayleen Torres Maldonado

A Thesis submitted in partial fulfillment of

the requirements for the degree of

Master of Science

(Atmospheric and Oceanic Sciences)

at the

University of Wisconsin-Madison

May 2023

Abstract

Processes Governing the Evolution of Moist Static Energy in Developing and Non-developing African Easterly Waves

by Kayleen Torres Maldonado

It is well known that African easterly waves (AEWs) occasionally develop into tropical cyclones. However, the processes leading to development are not well understood. To this end, we examine a 38-year climatology of AEW tracks sorted into developing (DAEWs) and non-developing (NDAEWs) waves. Regional composites over the 40°W-20°E domain are constructed as well as wave-centered composites for tracks in the eastern Atlantic (40°W-10°W) and west African monsoon regions (10°W-20°E). DAEWs are found to occur over a background state that is more humid and exhibits a steeper meridional moist static energy (MSE) gradient, especially over the west African monsoon (AM). Relative to NDAEWs, DAEWs over the AM have heavier precipitation that is shifted slightly westward of the vorticity center. DAEWs over the east Atlantic (EA) also precipitate more heavily, but the precipitation in this region is co-located with the center of circulation. When examining the column MSE budget of DAEWs and NDAEWs, it is found that the main difference between DAEWs and NDAEWs is a reduction in drying by horizontal MSE advection to the east of the vortex center. Over the EA basin, DAEWs exhibit stronger radiative heating and surface fluxes. It is hypothesized that it is the more humid environment that differentiates DAEWs from NDAEWs, which suppresses drying by

horizontal moisture advection, allowing the DAEWs to become better organized as they transit the African monsoon and the east Atlantic.

Acknowledgements

While the last three years have been nothing short of challenging, they have also been filled with learning, growth, and significant experiences that I will carry with me throughout my career. I am deeply thankful to everyone that has been part of my process and contributed to my personal and academic growth. I would first like to thank my advisor, Dr. Ángel F. Adames Corraliza, for his unwavering support and guidance throughout my master's program. His expertise and patience have been invaluable to me and have played a crucial role in the success of this thesis. I cannot express how appreciative I am of Dr. Adames for not only being a great research advisor but also a great life mentor. I am also thankful to the Large-Scale Tropical Dynamics research group (Victor C. Mayta, Rosa Vargas Martes, Haochang "HC" Luo, Qiao-Jun Lin, Chelsea Snide, and Becca Hall) for their continued support and friendship. They have made my time in graduate school more memorable. I will always remember our insightful conversations, group meetings, lunches, and of course, our mischiefs in the office.

I am also grateful for my coding mentor, Dr. Hannah Zanowski for all the help and guidance she provided with the construction of the project algorithm, and for always saving me time and trouble with my codes. I would like to acknowledge Drs. Ángel F. Adames, Victor C. Mayta, and Kelly Nuñez Ocasio for their contributions to this research and help with my first publication. I want to also thank my committee members, John Martin and Larissa Back for their insights and comments on this thesis work.

Lastly, I would also like to thank my family for their love and support during this process, and my husband for always reminding me what I am capable of. Without them, this journey would not have been possible.

Contents

List of Figures

Chapter 1

Introduction

1.1 African Easterly Waves

African easterly waves (AEWs) are synoptic-scale disturbances that propagate westward during the boreal summer months and the West African monsoon season (Burpee, 1972, Carlson, 1969). It is well documented that AEWs are related to Atlantic tropical cyclones (TCs) as AEWs can serve as TC precursors (i.e., Avila et al., 2000, Landsea, 1993). Barotropic and baroclinic instabilities—arising from the reversal of the background potential vorticity (PV) meridional gradient over Africa—have been thought to be the main processes responsible for the generation and energetics of AEWs (Charney and Stern, 1962, Norquist et al., 1977, Pytharoulis and Thorncroft, 1999). More recently, studies have emphasized the role of convection and thermodynamics in the generation

and growth of AEWs (Adames and Ming, 2018, Cohen and Boos, 2016, Diaz and Boos, 2021).

Using an idealized modeling framework, Thorncroft et al. (2008) showed that diabatic heating close to the African easterly jet (AEJ) can aid AEW genesis. Also using an idealized framework, Cornforth et al. (2009) showed that including moist processes can increase barotropic conversions and AEJ development that in turn produces stronger AEWs when compared to the controlled (dry) experiment. In addition to wave initiation and growth, moist processes also play an important role in TC genesis.

Climatologically, developing AEWs (DAEWs; those that become TCs) tend to have stronger low-level circulation associated with more convective activity over the west coast of Africa and the main development region (MDR), compared to non-developing AEWs (NDAEWs; Hopsch et al., 2010, Kiladis et al., 2006). DAEWs also have higher low- to mid-level relative humidities than NDAEWs (Brammer and Thorncroft, 2015). In West Africa, DAEWs are more likely to have a larger number of mesoscale convective systems (MCSs), which are more intense and with larger cloud regions, providing more diabatic heating of the eddy at wave-scale vortex than NDAEWs (i.e., Núñez Ocasio et al., 2020). It is becoming increasingly evident that the co-location of moisture and convection with the wave-scale AEW eddy is essential for Atlantic TC formation (i.e., Núñez Ocasio et al., 2020, Semunegus et al., 2017, Tomassini et al., 2017). Over western Africa and the eastern Atlantic, Núñez Ocasio et al. (2020) found that MCSs of DAEWs are more likely to be in phase with the AEW vortex than MCSs of NDAEWs and they proposed that this

phasing is observational evidence that moisture-vortex instability (MVI), as described by Adames and Ming (2018) and Adames (2021) (or the rotational stratiform instability by Russell et al. (2020)), can serve as a mechanism for AEW growth and subsequent TC genesis. In both mechanisms, the AEW circulation creates a favorable environment for convection through large-scale moistening, and the subsequent convection strengthens the circulation through vortex stretching.

1.2 Moist Static Energy

While all these previous results suggest an important role in interactions between moisture, convection, and the large-scale circulation in AEWs, many gaps in our understanding of these remain (Wing et al., 2019b). One way that we can potentially elucidate some of these interactions is through the application of the moist static energy (MSE) and its budget (Back and Bretherton, 2005, Emanuel et al., 1994, Yanai et al., 1973). Previous studies have employed MSE budgets to understand the thermodynamics of tropical waves (Adames and Ming, 2018, Andersen and Kuang, 2012, Mayta and Adames, 2023, Mayta et al., 2022, Mayta and Adames Corraliza, 2023), and to understand TC genesis in idealized models (Wing, 2022, Wing et al., 2016, 2019b). These studies have shown that horizontal MSE advection is important for the destabilization and propagation of tropical depression-like waves such as easterly waves. They have also shown the importance of cloud-radiative heating in the growth of these waves and in TC genesis. Furthermore, other studies have shown an increase in column moisture and MSE during TC genesis

(Núñez Ocasio and Rios-Berrios, 2023, Wing et al., 2019a). Despite these findings, the MSE budget has not been widely used to understand AEW behavior.

1.3 Research Questions

In this study, we examine the MSE distribution and its tendency budget to answer the following questions:

Q1: Is the distribution of background MSE different during the passage of DAEWs and NDAEWs?

Q2: Can changes in the background state explain the differences in the MSE budget between DAEWs and NDAEWs?

Q3: Are the processes that govern the evolution of MSE different in DAEWs and NDAEWs?

In order to answer these questions, we will employ the compositing methods of Núñez Ocasio et al. (2021) to assess the role of each of the MSE budget terms in the development and TC genesis of AEWs, and to elucidate other thermodynamic differences in DAEWs and NDAEWs. Consistent with Núñez Ocasio et al. (2021), DAEWs in this 38-yr climatology show overall stronger, vertically stacked circulations compared to NDAEWs. These stronger circulations are due to higher humidity surrounding the DAEWs –likely associated with a stronger monsoon– which reduces drying by horizontal MSE advection,

consistent with previous studies (Adames and Ming, 2018, Mayta and Adames Corraliza, 2023, Núñez Ocasio and Rios-Berrios, 2023).

Chapter 2

Data and Methods

2.1 Data

A 38-yr June–October (1980–2017) climatology of DAEWs and NDAEWs is used in this work. We perform a similar AEW analysis to that in Núñez Ocasio et al. (2021), using the AEW track dataset of Cheng et al. (2019). The track data uses European Centre for Medium-Range Weather Forecasts (ECMWF) interim reanalysis (ERA-Interim; Dee et al., 2011). It follows the tracking method used in Brammer and Thorncroft (2015) that matches AEW tracks with the National Hurricane Center Atlantic Hurricane Database, version 2 (HURDAT2; Landsea et al., 2014), to identify DAEWs. The total number of DAEWs and NDAEWs is 189 and 5246, respectively, and the number of DAEWs and NDAEWs included in each composite region is shown in Fig. 2.1. Differently from the work done in Núñez Ocasio et al. (2021), both DAEWs and NDAEWs are considered

throughout their lifetime, but limiting them to the time steps that the waves were within the boundaries of the regions of the analyzed domain. What differentiates DAEWs from NDAEWs is that DAEWs undergo TC genesis (become tropical depression) at some point in their lifetime, while NDAEWs never do.

To assess the thermodynamical characteristics associated with AEWs, ERA-5 (Hersbach et al., 2019) atmospheric fields are used to create AEW-following composites. Both datasets used (AEW track data and ERA-5) have a temporal resolution of 6 h and a horizontal resolution of 0.5°. A June–October climatology of AEWs is used considering that it represents the months of highest TC activity in the north Atlantic, and therefore providing a bigger pool of DAEWs tracks.

2.2 Geographic composites

Geographical composites are a good starting point to understanding the differences between DAEWs and NDAEWs and are hence used to evaluate the environmental conditions surrounding the AEWs. The domain region for these composites encompasses latitudes from 5°S to 30°N and longitudes from 40°W to 20°E. The number of DAEWs and NDAEWs included in these composites is shown in the top panel of Fig. 2.1. As in Núñez Ocasio et al. (2021), the geographic composites are built by grouping the DAEWs and NDAEWs periods that the wave trough center is positioned within the domain boundaries, and calculating the time-average period over the region. Therefore, the composite

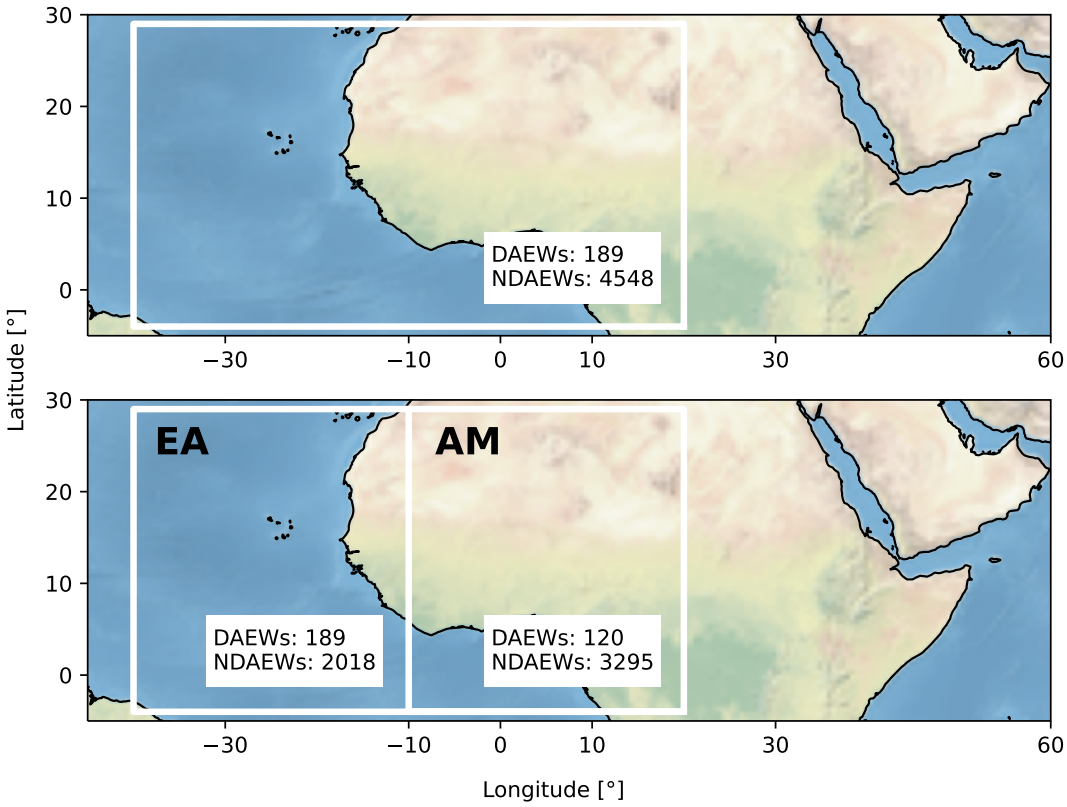

FIGURE 2.1: (top) Domain region for geographic composites. The white-outlined box represents the composite boundaries. (bottom) Domain region for wave-centered composites. The white-outlined boxes represent regions identified as AM (African Monsoon) and EA (East Atlantic). The total numbers of DAEWs and NDAEWs used for each composite region are shown in the lower right corner of each region.

means in Fig. 3.1 are the mean over all of the time-averaged AEW periods. These composites are then used to understand the environmental thermodynamics of DAEWs and NDAEWs as they move over the continent and off the west African Coast.

2.3 Wave-centered composites

A series of wave-centered composites were calculated to assess the environment near the center of the AEW trough. These composites are performed by computing the spatial mean over the time-averaged AEW periods, but restricted to the trough center and grouped in smaller regions. The bottom panel in Figure 2.1 shows the African Monsoon (AM; 10°W to 20°E) and the East Atlantic (EA; 40°W to 10°W), and both regions encompass latitudes from 5°S to 30°N. The number of DAEWs and NDAEWs used in each composite is shown in white boxes. For a wave to be part of a region, the trough center must be located at least one time step within that region. For instance, a wave that develops in the AM region and reaches the EA, counts as a DAEW in both regions. A wave that moves over the AM but does not develop until it reaches the EA, counts as a NDAEW in the AM but as DAEW in the EA.

Chapter 3

Large-scale thermodynamics

The column-integrated MSE is defined as,

$$\langle m \rangle = \frac{1}{g} \int_{p_t}^{p_s} (\underbrace{C_p T + \Phi}_{DSE} + L_v q) dp \tag{3.1}$$

where p_t is the pressure at the top of the atmosphere, p_s is the pressure at the surface, C_p is the specific heat at constant pressure, and q is the water vapor mixing ratio. MSE is approximately conserved under moist adiabatic processes, and its column integration is unaffected by convection (Emanuel et al., 1994). For this reason, column-integrated MSE has been extensively used as a thermodynamic representation of the tropical atmospheric column (Maloney, 2009).

The mean state thermodynamic conditions over tropical West Africa and East Atlantic are shown in Fig. 3.1. The precipitation signature is significant along the 10°N latitude in both DAEWs (Fig. 3.1a) and NDAEWs (Fig. 3.1e), especially off the west African Coast. However, when DAEWs are active, precipitation shifts poleward and extends over a wider area. A similar pattern was observed in the MSE distribution, particularly over the eastern Atlantic. Differences in precipitation (Fig. 3.1i) show that DAEWs exhibit a larger rainfall signature than NDAEWs. Considering the differences between the MSE composites (Fig. 3.1j) we see that the mean MSE is larger to the north of DAEWs than NDAEWS. It is also smaller to the south, again indicating that the mean meridional MSE gradient is stronger for the DAEWs. It is worth noting that precipitation is maximum in regions where the horizontal MSE gradient is strong.

Since the MSE is a measure of a parcel's internal, potential, and latent energy, it can conveniently be used to understand temperature and moisture contributions. Thus, composites of column dry static energy (DSE) and column latent energy, here represented as the total column water vapor (TCWV), are evaluated to understand the individual contributions to the column-integrated MSE. The horizontal distribution of the DSE in the DAEWs (Fig. 3.1c) and NDAEWs (Fig. 3.1g) resemble each other, but the difference composite (Fig. 3.1k) suggest that DAEWs exhibit anomalous warmth north of 10°N. The moisture signature is apparent from the TCWV composites in both DAEWs (Fig. 3.1d) and NDAEWs (Fig. 3.1h). The differences between the TCWV composites (Fig. 3.1l) show that the environment in which DAEWs propagate is more humid than

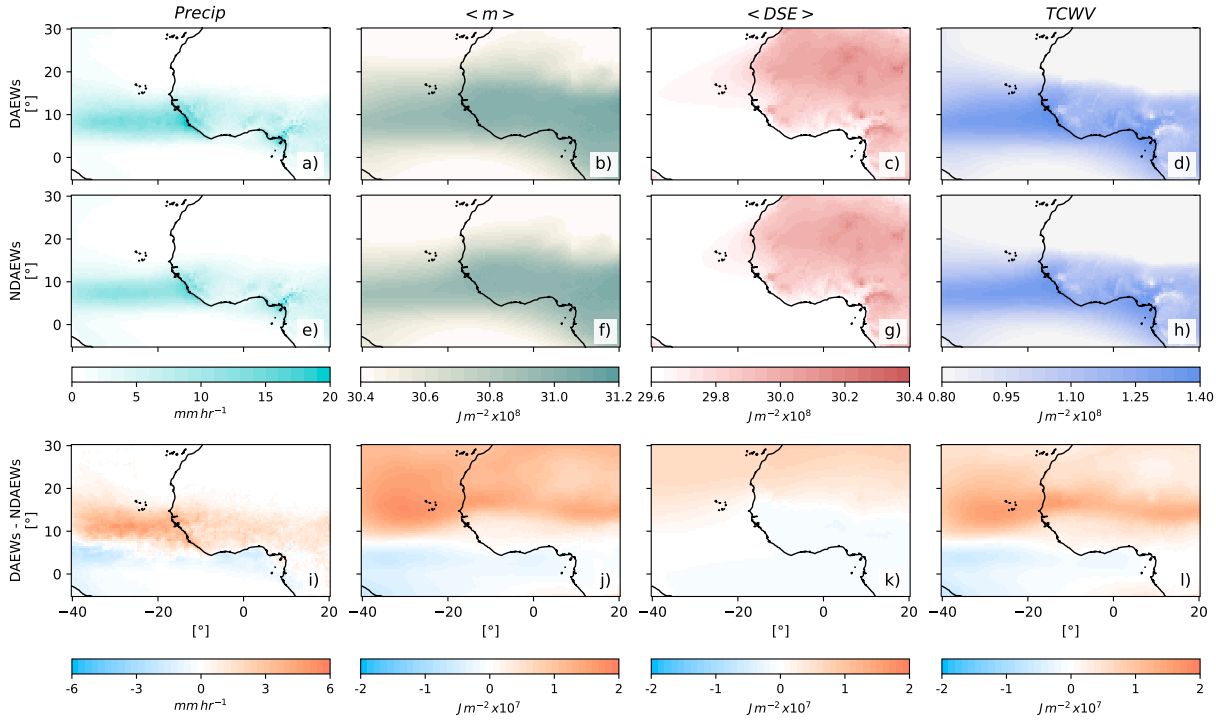

FIGURE 3.1: Geographic composites of (left) precipitation rate, (left-center) column-integrated MSE, (right-center) column-integrated DSE and (right) TCWV for (a)–(d) DAEWs and (e)–(h) NDAEWs. (i)–(l) The difference between composites (DAEWs - NDAEWs).

NDAEWs, especially off the west African Coast. Examination of the difference composites (Fig. 3.1j-l), it is evident that the horizontal distribution of MSE closely follows both the moisture and temperature distributions, but moisture contributes the most to the MSE gradient over the region.

Chapter 4

Wave structure and the surrounding environment

4.1 African Monsoon region

In this section, we examine the thermodynamic environment near the vortex center of the two types of AEWs. Figure 4.1 shows wave-centered composites of DAEWs and NDAEWs over the AM region. We see that DAEWs in this region exhibit a region of enhanced precipitation located centered $\sim 2^{\circ}$ to the west of the 850 hPa trough axis (Fig. 4.1a). MSE depicts its maximum values to the north and northeast of the DAEW center, and the vortex center is located in a region where the meridional MSE gradient is strong (Fig. 4.1b). In contrast, TCWV is the largest to the southwest of the DAEW, and its

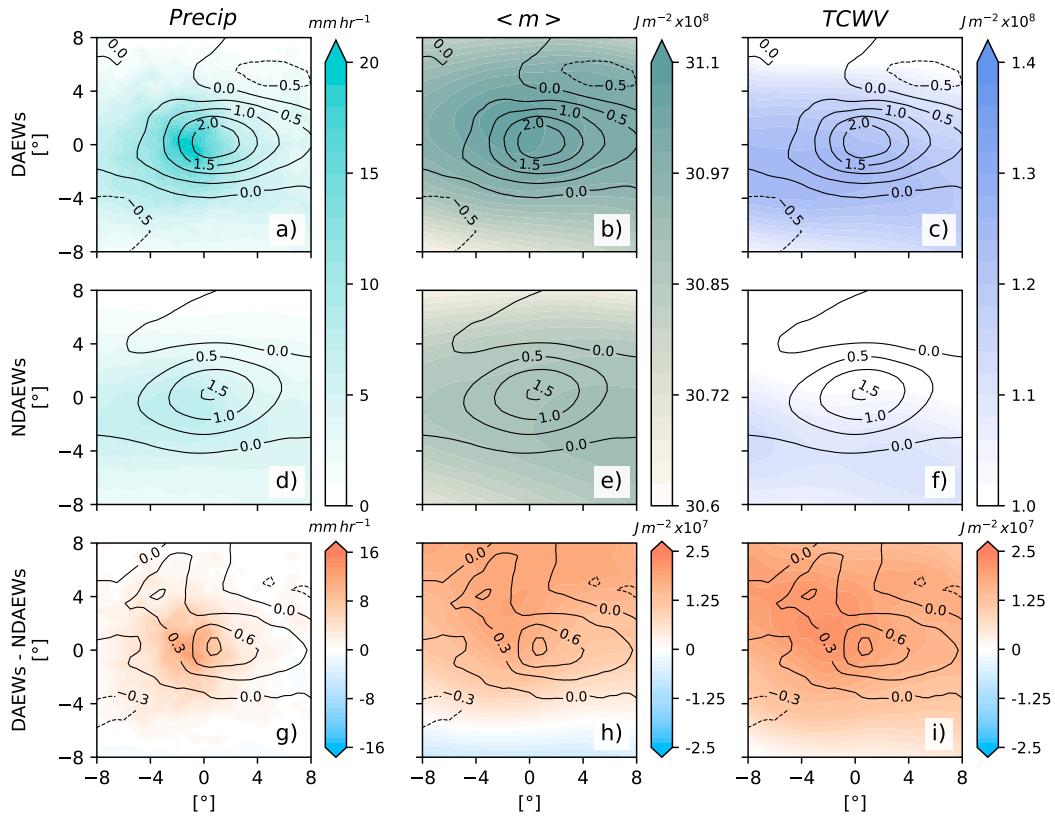

FIGURE 4.1: Wave-centered composites for African Monsoon region of (left) precipitation rate, (center) column-integrated MSE, (right) TCWV for (a)–(c) DAEWs and (d)–(f) NDAEWs. (g)–(i) The difference between composites (DAEWs - NDAEWs). Labeled solid black contours are 850-hPa relative vorticity ($\times 10^{-5} s^{-1}$).

gradient is in the reverse direction as the MSE gradient (Fig. 4.1c). This result indicates that there is a substantial horizontal DSE gradient in the DAEW.

NDAEWs exhibit weaker vorticity and less rainfall than the DAEWs (Fig. 4.1d). The rainfall is also shifted further south and west of the wave axis when compared to DAEWs. Notably, the MSE is weaker and exhibits a maximum to the southeast, rather than to the north (Fig. 4.1e). The strong meridional MSE gradient observed in DAEWs is absent in NDAEWs. The thermodynamic environment is also drier in NDAEWs, evidenced by the

smaller TCWV values seen in Fig. 4.1f. The TCWV maximum is also located further south in NDAEWs than in DAEWs.

The bottom row of Fig. 4.1 confirms the differences discussed above but also reveals further details about the contrast between the DAEW and NDAEW environments. For example, we see a waviness in the MSE differences, with MSE being higher to the west of the wave center of DAEWs than to the east. A similar result is also seen in the TCWV anomalies, with the largest difference between DAEWs and NDAEWs centered 3°W and 2°N of the wave axis. Collectively, these results indicate that the DAEW thermodynamic environment is characterized by a stronger horizontal MSE gradient and a more humid environment.

4.2 East Atlantic region

Figure 4.2 shows the near-through thermodynamic environment of the two types of AEWs over the EA region. Once waves reach this region, they exhibit a more organized and strong vortex in both DAEWs and NDAEWs. Similar to the AM region, DAEWs present a region of enhanced precipitation that is now more co-located with the vortex center, although slightly to the south of the trough axis (Fig. 4.2a). In this region, we still see a maximum MSE slightly to the northeast, but nearest to the vortex center of DAEWs (Fig. 4.2b). However, the MSE gradient is not as strong as in the AM region. This is because the largest values of DSE are over the continent, contributing to the large steep in meridional MSE gradient over the AM. Consistent with the precipitation distribution,

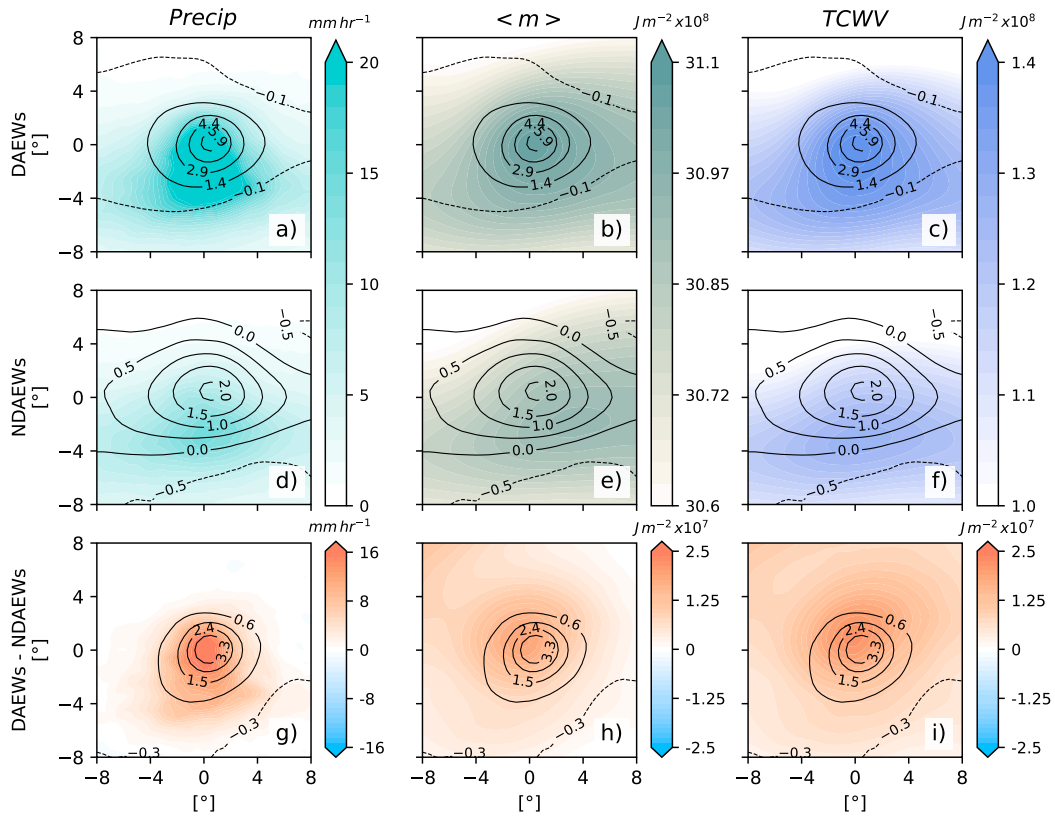

FIGURE 4.2: As in Fig. 4.1 but for East Atlantic region.

the TCWV in the DAEWs is now more centralized to the vortex center but with its maximum shifted moderately to the southwest (Fig. 4.2c).

As in the AM, in this region, the NDAEWs show weaker vorticity and less precipitation associated with them compared to the DAEWs (Fig. 4.2d). While we see increased precipitation in this region for the NDAEWs, the rainfall is still shifted further to the south of the wave axis when compared to DAEWs. The MSE gradient is also weaker and the MSE maximum is largely displaced to the east (Fig. 4.2e). While there is an increase in moisture over the EA, the NDAEWs still present a drier environment than DAEWs

and this is apparent by the smaller values of TCWV shown in Fig. 4.2f. The TCWV in the NDAEWs is also more to the south than for DAEWs.

When looking at the differences between DAEWs and NDAEWs in Fig. 4.2, it is evident that DAEWs exhibit larger values of MSE and humidity, which results in enhanced precipitation compared to NDAEWs. It is also visible that, in this region, the AEWs not only present a more organized vortex structure but also a more defined distribution of these thermodynamic fields.

4.3 Vertical structure

To analyze the vertical structure of the AEWs, we show in Fig. 4.3 composites over the AM and EA regions for DAEWs and NDAEWs with relative vorticity contours at the 850 and 500 hPa levels. In the AM region, we see that for the DAEWs, the vorticity at the mid-levels is slightly shifted to the west of the 850 hPa vorticity (Fig. 4.3b), consistent with previous studies (Núñez Ocasio et al., 2021, 2020, Russell and Aiyyer, 2020, Russell et al., 2020). This slight tilt in the vortex structure is inconsistent with moist baroclinic growth since this mechanism requires the AEWs to tilt eastward with height over the AM region (Adames, 2021, Cohen and Boos, 2016). That the tilt is in the opposite direction indicates that other processes may be responsible for the growth of AEWs. The precipitation is also leading the low-level vortex. This feature is due to strong wind shear in the region advecting positive vorticity down shear of the wave, causing upward motion

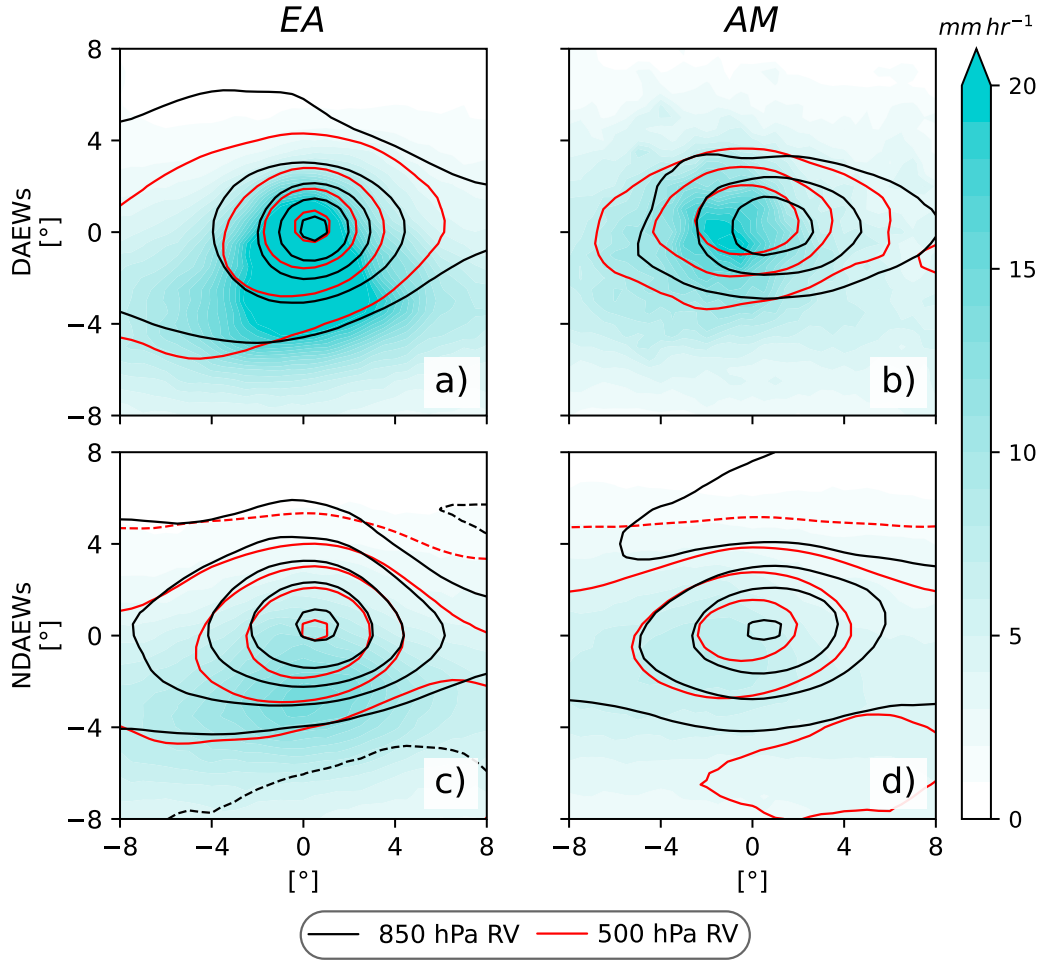

FIGURE 4.3: Wave-centered composites for regions (left) East Atlantic and (right) African Monsoon of precipitation rate. Relative vorticity ($\times 10^{-5} s^{-1}$) at 850 (black contours) and 500 (red contours) hPa for (a)–(b) DAEWs and (c)–(d) NDAEWs.

(Kiladis et al., 2006). For NDAEWs, the shift to the west in the mid-levels is still present but not so evident as the vortex seems to be more vertically aligned (Fig. 4.3d).

Once the waves reach the EA region, we find a vortex structure that is more vertically aligned for both DAEWs and NDAEWs. For the DAEWs, the 500 hPa vortex seems to be stacked over the 850 hPa vortex (Fig. 4.3a). In the NDAEWs composite, there is still a slight shift of the mid-level vortex to the southwest, but we see a more vertically

aligned structure than in the AM region (Fig. 4.3c). This structure suggests that growth by barotropic or MVI is possible in either DAEWs and NDAEWs, but it is unlikely that baroclinic growth is occurring in either.

Chapter 5

MSE Budget Analysis

5.1 MSE budget composites

The column-integrated MSE budget is defined as in Yanai et al. (1973),

$$\frac{\partial \langle m \rangle}{\partial t} = -\langle \mathbf{v} \cdot \nabla m \rangle - \left\langle \omega \frac{\partial m}{\partial p} \right\rangle + \langle Q_r \rangle + SF \tag{5.1}$$

where $\langle m \rangle$ is the column MSE defined in Eq. (3.1). The left-side term in Eq. (5.1) is the MSE tendency. The first and second terms on the right side of the equation represent the horizontal and vertical advection of MSE, respectively. The other two terms in Eq. (5.1) are the MSE source terms: the radiative heating rate and the surface fluxes, which include the surface latent heat flux ($L_v E$) and the surface sensible heat flux (SH).

To better understand the processes governing the thermodynamics of DAEWs and NDAEWs, it is instructive to examine the contribution of each budget term to the evolution of MSE. Fig. 5.1 shows wave-centered composites of MSE budget terms for AEWs over the AM region. In DAEWs, we see an MSE tendency roughly in quadrature with the precipitation, with MSE increasing to the west and decreasing to the east (Fig. 5.1a). In contrast, the MSE tendency in NDAEWs is much weaker and does not show the horizontal structure and coherence that is observed in DAEWs (Fig. 5.1b), which is most clearly seen when we take their differences (Fig. 5.1k).

We will now examine the terms on the right-hand side of Eq. (5.1). In both DAEWs and NDAEWs, we see that horizontal MSE advection predominantly dampens the MSE field. However, this damping is weakened, even reversed, to the east of the composite DAEW (5.1b). In contrast, horizontal MSE advection becomes more negative to the east of the NDAEWs (5.1l). This difference largely accounts for the difference in the MSE tendency that we see in Fig. 5.1k. The other terms, vertical MSE advection, radiative heating, and surface fluxes, are more in phase with the precipitation in AEWs. Most notably, all three processes are stronger in DAEWs (5.1c-e). When we take the difference we see stronger damping by vertical MSE advection and a positive contribution from radiative heating near the maximum precipitation in DAEWs. This result is consistent with the idea that radiative heating plays an important role in TC development (Ruppert et al., 2020, Wing, 2022). Given that the surface fluxes in this region are mostly dominated by sensible heat, this term is contributing negatively to the MSE tendency.

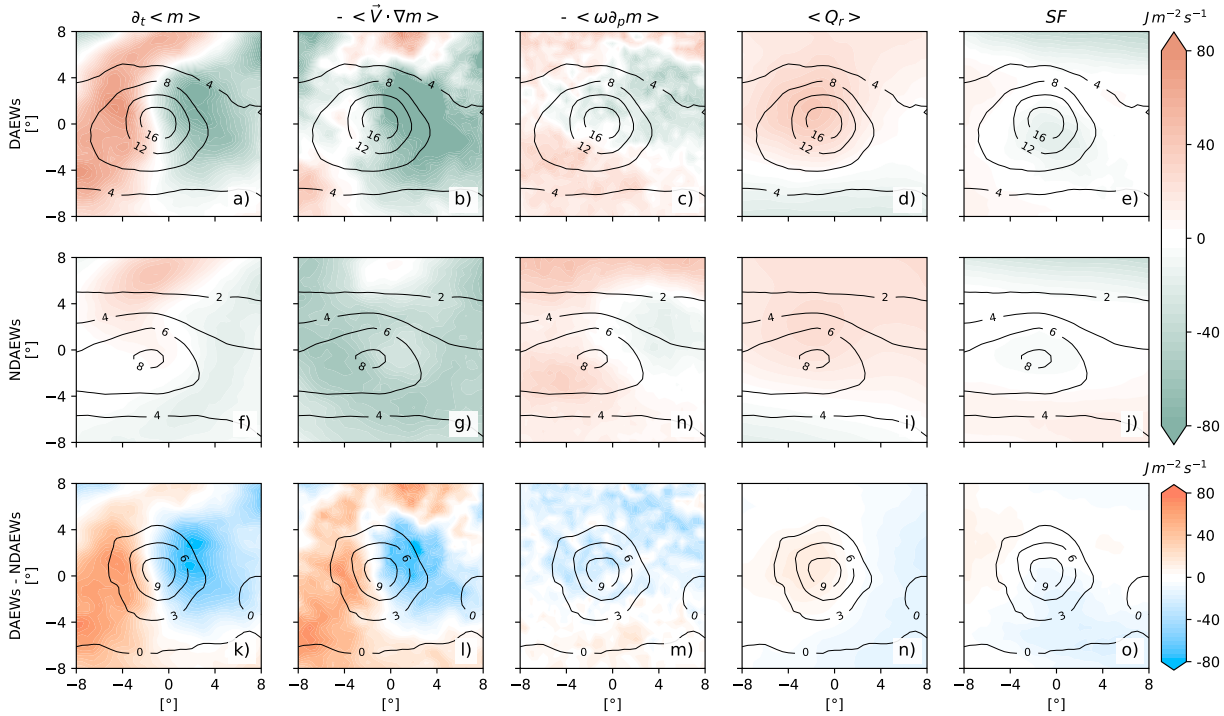

FIGURE 5.1: Wave-centered composites for African Monsoon region of MSE budget terms. (first column) MSE tendency, (second column) horizontal MSE advection, (third column) vertical MSE advection, (fourth column) radiative heating, and (fifth column) surface fluxes for (a)-(e) DAEWs and (f)-(j) NDAEWs. (k)-(o) the difference between composites (DAEWs - NDAEWs). Labeled solid black contours are precipitation rate ($mmhr^{-1}$).

Figure 5.2 shows the MSE budget composites for the EA region. For the DAEWs we see a similar spatial distribution of MSE tendency than what we found in the AM region, but more enhanced (Fig. 5.2b). However, in the NDAEWs we see a much more increased MSE tendency from what was seen in the AM, with a more coherent horizontal structure (Fig. 5.2f). When taking the differences between DAEWs and NDAEWs we see that DAEWs have stronger MSE increasing to the west and decreasing to the east (Fig. 5.2k).

It is evident that the MSE horizontal advection is the term that predominantly contributes to the MSE tendency in both DAEWs and NDAEWs. In contrast to the AM region

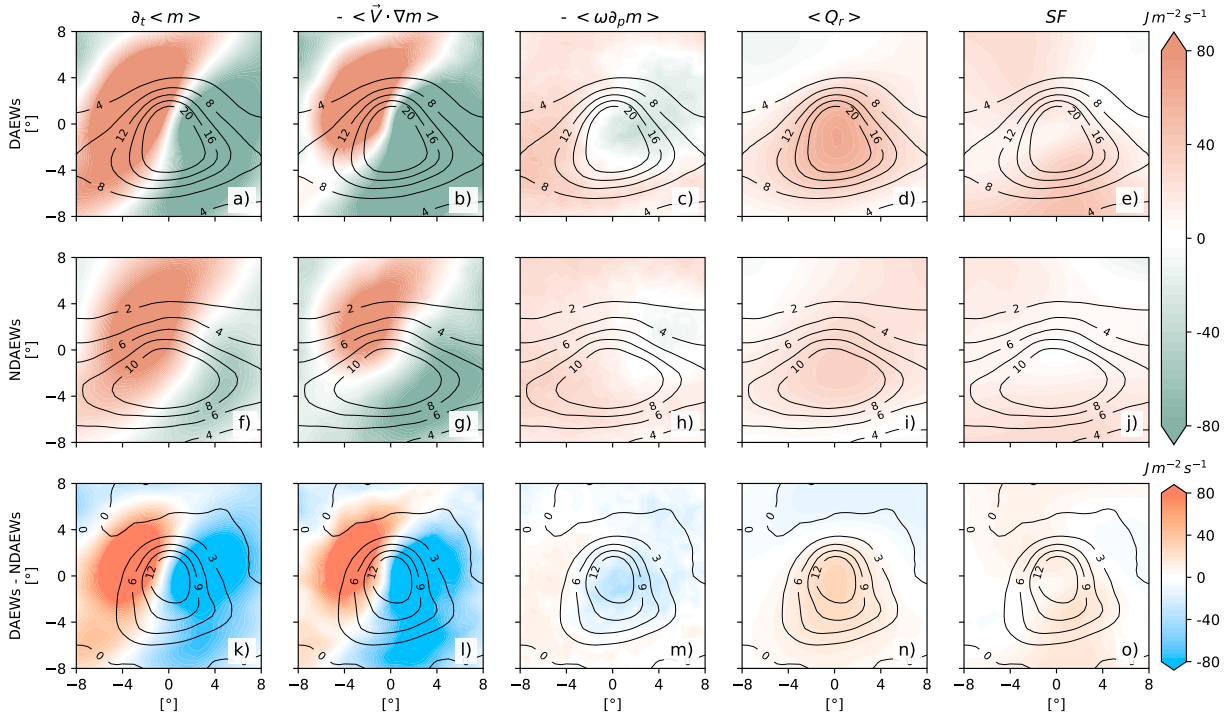

FIGURE 5.2: As in Fig. 5.1 but for East Atlantic region.

where we mostly saw the MSE advection damping the MSE field, in the EA region, we now see that it promotes MSE increase to the north-northwest, and decrease to the south-southeast of the wave. In the EA region, we see the formation of a dipole structure in the MSE advection that was not present in the AM region, especially in the NDAEWs. The vertical MSE advection, radiative heating, and surface fluxes are stronger for DAEWs. We see increased radiative heating in the EA region, particularly for the DAEWs, with the maximum constricted to the precipitation signature (Fig. 5.2d). This feature is not so evident in the NDAEWs radiative heating structure (Fig. 5.2i). The surface fluxes also increase in the EA, as the waves move across the ocean.

5.2 Processes that control the growth and propagation of AEWs

In order to more objectively quantify the relative contributions of each MSE term to the propagation and maintenance of the two AEW types, the spatial pattern of each budget term is projected onto the MSE tendency and the column-integrated MSE, i.e.,

$$\mathrm{Proj}(F, \langle m \rangle) = \frac{||F \cdot \langle m \rangle||}{||\langle m \rangle \cdot \langle m \rangle||} \tag{5.2a}$$

$$\mathrm{Proj}(F, \partial\langle m \rangle/\partial t) = \frac{||F \cdot \partial\langle m \rangle/\partial t||}{||\partial\langle m \rangle/\partial t \cdot \partial\langle m \rangle/\partial t||} \tag{5.2b}$$

where F denotes each individual term in Eqs. (5.1), and $||\cdot||$ implies an areal average from the wave-centered composites. The positive and negative projections in Eq. (5.2a) correspond to contributions to the amplification and decay of the disturbance, respectively. Similarly, Eq. (5.2b) measures how much terms contribute to the westward propagation of the AEWs over the two regions considered for the analysis.

The mechanisms responsible for the maintenance and propagation of AEWs over the AM and EA are illustrated in Figs. 5.3. The MSE budgets have large residuals, which lends less confidence to our conclusions, especially over the AM region. Note that the MSE budget residuals for the convectively coupled waves over the western hemisphere

have been recently discussed in Mayta and Adames (2023). The large residuals indicate that there is a missing moistening source in the AEWs convection associated with the advection terms. It is worth noting the obvious underestimation of the role of the vertical MSE (Fig. 5.3). These results are in agreement with Mayta and Adames (2023), who also found that the role of MSE vertical advection is significantly underestimated when the reanalysis is compared to observations (see their Fig. 10).

Consistent with the discussions in the previous section and what has been stated in many previous studies, the leading term associated with amplifying AEWs is longwave radiative heating (Figs. 5.3a, b). Longwave radiative heating contributes significantly to the growth of the system because the upper-level cirrus clouds act as a blanket, amplifying the system. This modulation was observed when the system was completely developed in the EA region (Fig. 5.3a). In contrast, horizontal MSE advection yields a negative contribution, especially when the wave propagates over land (Fig. 5.3b). We hypothesize that reanalysis does not show a good performance over the continent and overestimates the contribution of horizontal advection, which is also reflected in the large residual value observed over AM. When the wave reaches the Atlantic Ocean, the horizontal MSE advection has a near-zero contribution. This result is in agreement with Mayta and Adames Corraliza (2023), who found that the horizontal advection of the MSE by anomalous meridional winds (that contributes to the growth) has nearly the same magnitude as the horizontal advection of the MSE by zonal mean winds (that contributes to the damping) trying to cancel each other. Surface fluxes, on the other hand, contribute non-negligible to

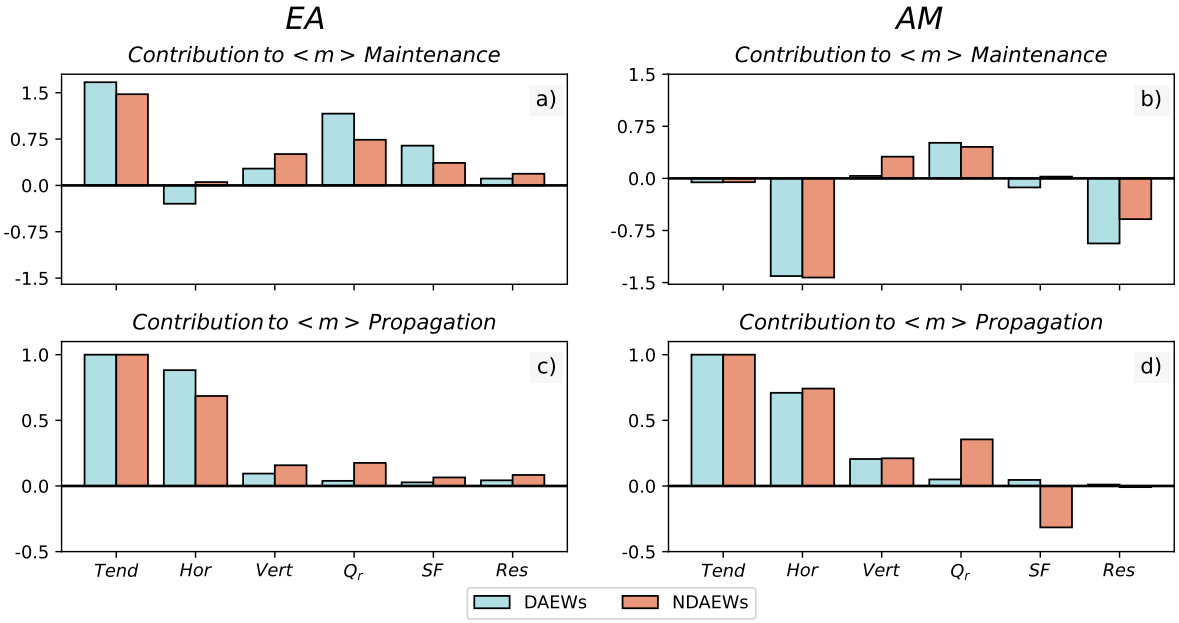

FIGURE 5.3: Area-weighted projection of the column-integrated right-hand side terms in Eq. (5.1) to the maintenance (top panels) and propagation (bottom panels) of the East Atlantic (EA) and African Monsoon (AM) easterly waves. Light green bars are for developers African easterly waves (DAEWs) and orange for non-developers African easterly waves (NDAEWs). Area-average weighted projections are over 5°S–30°N,40°W–10°W for EA and 5°S–30°N,10°W–20°E for AM.

DAEWs' growth when the wave reaches a relatively mature stage over the open ocean (light green bar in Fig. 5.3a).

The total MSE tendency associated with the AEWs, which explains their westward propagation, is primarily modulated by horizontal MSE advection. This term contributes to over 50% of the column MSE tendency in both regions (Figs. 5.3c, d). Other terms contribute little to wave propagation.

Chapter 6

Summary and Conclusions

Motivated by previous studies showing that MSE can be used to understand TC genesis (Wing, 2022, Wing et al., 2016, 2019b), this study sought to better understand the thermodynamic processes that distinguish developing (DAEWs) and non-developing (NDAEWs) waves. To this end, we used the methods of Núñez Ocasio et al. (2021) to create regional and wave-centered composites. We also examined the MSE distribution, including its individual contributions, as well as its tendency budget to answer the three questions posed in Chapter 1. Below are the answers to these questions based on the results discussed in Chapters 3-5.

Q1: The distribution of background MSE is different during the passage of DAEWs and NDAEWs.

The largest difference we found in the thermodynamic environment surrounding DAEWs and NDAEWs is the higher moisture surrounding the DAEWs. Higher moisture is seen in the geographical composites (Fig. 3.1), and on the wave-centered composites (Figs. 4.1 and 4.2). Dry static energy (DSE) exhibits a larger gradient, and together with the increased moisture, it seems likely that changes in both moisture and DSE are the result of northward shifted and stronger African Monsoon, consistent with Núñez Ocasio et al. (2021). However, it is clear that increased moisture contributes most to the changes in moist static energy (MSE), as seen in the difference plots of both geographical (Fig. 3.1j,l) and wave-centered composites (Fig. 4.1 and 4.2 h,i).

Q2: Changes in the background state explain the differences in the MSE budget between DAEWs and NDAEWs.

But how does the more humid environment favor AEW development? The biggest clue comes from examining the wave-centered composites in Fig. 4.1 and 4.2. Even in these composites, we see higher precipitation rates in DAEWs that are co-located with and surrounded by high values of column-integrated water vapor of $\sim$ 50 mm. These values are up to 30% higher than those obtained for NDAEW. This higher moisture is likely the main reason why drying by horizontal MSE advection is weakened to the west of the wave axis in DAEWs (Figs. 5.1 and 5.2), which in turn allows other thermodynamic processes to enhance DAEW organization.

Q3: The processes that govern MSE evolution are more coherent in DAEWs than in NDAEWs.

The processes that are responsible for the growth and propagation of DAEWs are clear, especially when the wave is over the ocean (left panels in Fig. 5.3a,c). Longwave radiative heating and surface fluxes are responsible for the maintenance of the column moisture anomalies associated with DAEWs in the EA (Fig. 5.3a). Horizontal MSE advection, on the other hand, is largely the main process responsible for the westward propagation of the DAEWs in both regions (Fig. 5.3c,d).

The results presented in this work support the hypothesis that differences in moisture content between the two types of waves are a key factor that allows some thermodynamic processes to favor tropical cyclogenesis in DAEWs and not in NDAEWs. However, this study has several caveats. First, while the methodology used here can provide a useful starting point for understanding the processes that drive MSE development, it may not precisely quantify individual contributions. A more careful selection of DAEW cases should give us more insights into how these disturbances evolve and the various thermodynamic processes associated with them. The second is to use the field campaign data to complement the reanalysis data due to the strong residuals found. The results in Chapter 5 suggest that, in agreement with Mayta and Adames (2023), the convection of AEWs associated with advection conditions may lack a source of moistening. The reanalysis

performs poorly over the continent, overestimating the contribution of horizontal advection, which is reflected in the large residual. In addition, model simulations with a strong sensitivity to the moisture gradient should be the subject of future work.

Bibliography

Adames, Á. F., 2021: Interactions between water vapor, potential vorticity and vertical wind shear in quasi-geostrophic motions: Implications for rotational tropical motion systems. *Journal of the Atmospheric Sciences*, doi:10.1175/JAS-D-20-0205.1.

Adames, A. F. and Y. Ming, 2018: Interactions between Water Vapor and Potential Vorticity in Synoptic-Scale Monsoonal Disturbances: Moisture Vortex Instability. *Journal of the Atmospheric Sciences*, **75**, 2083–2106, doi:10.1175/JAS-D-17-0310.1.

Andersen, J. A. and Z. Kuang, 2012: Moist Static Energy Budget of MJO-like Disturbances in the Atmosphere of a Zonally Symmetric Aquaplanet. *Journal of Climate*, **25**, 2782 – 2804, doi:10.1175/JCLI-D-11-00168.1.

Avila, L. A., R. J. Pasch, and J.-G. Jiing, 2000: Atlantic tropical systems of 1996 and 1997: Years of contrasts. *Monthly Weather Review*, **128**, 3695 – 3706, doi:https://doi.org/10.1175/1520-0493(2000)128¡3695:ATSOAY¿2.0.CO;2.

Back, L. E. and C. S. Bretherton, 2005: The relationship between wind speed and precipitation in the pacific itcz. *Journal of climate*, **18**, 4317–4328.

Brammer, A. and C. D. Thorncroft, 2015: Variability and evolution of african easterly wave structures and their relationship with tropical cyclogenesis over the eastern atlantic. *Monthly Weather Review*, **143**, 4975 – 4995, doi:10.1175/MWR-D-15-0106.1.
URL https://journals.ametsoc.org/view/journals/mwre/143/12/mwr-d-15-0106.1.xml

Burpee, R. W., 1972: The origin and structure of easterly waves in the lower troposphere of north africa. *Journal of Atmospheric Sciences*, **29**, 77 – 90, doi:https://doi.org/10.1175/1520-0469(1972)029¡0077:TOASOE¿2.0.CO;2.

Carlson, T. N., 1969: Synoptic histories of three african disturbances that developed into atlantic hurricanes. *Monthly Weather Review*, **97**, 256 – 276, doi:https://doi.org/10.1175/1520-0493(1969)097¡0256:SHOTAD¿2.3.CO;2.

Charney, J. G. and M. E. Stern, 1962: On the stability of internal baroclinic jets in a rotating atmosphere. *Journal of Atmospheric Sciences*, **19**, 159 – 172, doi:https://doi.org/10.1175/1520-0469(1962)019¡0159:OTSOIB¿2.0.CO;2.

Cheng, Y.-M., C. D. Thorncroft, and G. N. Kiladis, 2019: Two contrasting african easterly wave behaviors. *Journal of the Atmospheric Sciences*, **76**, 1753 – 1768, doi:10.1175/JAS-D-18-0300.1.
URL https://journals.ametsoc.org/view/journals/atsc/76/6/jas-d-18-0300.1.xml

Cohen, N. Y. and W. R. Boos, 2016: Perspectives on Moist Baroclinic Instability: Implications for the Growth of Monsoon Depressions. *Journal of the Atmospheric Sciences*, **73**, 1767–1788, doi:10.1175/JAS-D-15-0254.1.

Cornforth, R. J., B. J. Hoskins, and C. D. Thorncroft, 2009: The impact of moist processes on the african easterly jet–african easterly wave system. *Quarterly Journal of the Royal Meteorological Society*, **135**, 894–913, doi:https://doi.org/10.1002/qj.414.

Dee, D. P., S. M. Uppala, A. J. Simmons, P. Berrisford, P. Poli, S. Kobayashi, U. Andrae, M. A. Balmaseda, G. Balsamo, P. Bauer, P. Bechtold, A. C. M. Beljaars, L. van de Berg, J. Bidlot, N. Bormann, C. Delsol, R. Dragani, M. Fuentes, A. J. Geer, L. Haimberger, S. B. Healy, H. Hersbach, E. V. Hólm, L. Isaksen, P. Kållberg, M. Köhler, M. Matricardi, A. P. McNally, B. M. Monge-Sanz, J.-J. Morcrette, B.-K. Park, C. Peubey, P. de Rosnay, C. Tavolato, J.-N. Thépaut, and F. Vitart, 2011: The ERA-Interim reanalysis: configuration and performance of the data assimilation system. *Quarterly Journal of the Royal Meteorological Society*, **137**, 553–597, doi:https://doi.org/10.1002/qj.828.

Diaz, M. and W. R. Boos, 2021: Evolution of Idealized Vortices in Monsoon-Like Shears: Application to Monsoon Depressions. *Journal of the Atmospheric Sciences*, **78**, 1207 – 1225, doi:10.1175/JAS-D-20-0286.1.

Emanuel, K. A., J. D. Neelin, and C. S. Bretherton, 1994: On large-scale circulations in convecting atmospheres. *Quarterly Journal of the Royal Meteorological Society*, **120**, 1111–1143.

Hersbach, H., W. Bell, P. Berrisford, A. Horányi, M.-S. J., J. Nicolas, R. Radu, D. Schepers, A. Simmons, C. Soci, and D. Dee, 2019: Global reanalysis: goodbye era-interim, hello era5, 17–24. doi:10.21957/vf291hehd7.

Hopsch, S. B., C. D. Thorncroft, and K. R. Tyle, 2010: Analysis of African Easterly Wave Structures and Their Role in Influencing Tropical Cyclogenesis. *Monthly Weather Review*, **138**, 1399–1419, doi:10.1175/2009MWR2760.1.

Kiladis, G. N., C. D. Thorncroft, and N. M. J. Hall, 2006: Three-dimensional structure and dynamics of african easterly waves. part i: Observations. *Journal of the Atmospheric Sciences*, **63**, 2212–2230, doi:10.1175/JAS3741.1.

Landsea, C. W., 1993: A climatology of intense (or major) atlantic hurricanes. *Monthly Weather Review*, **121**, 1703 – 1713, doi:https://doi.org/10.1175/1520-0493(1993)121¡1703:ACOIMA¿2.0.CO;2.

Landsea, C. W., A. Hagen, W. Bredemeyer, C. Carrasco, D. A. Glenn, A. Santiago, D. Strahan-Sakoskie, and M. Dickinson, 2014: A reanalysis of the 1931–43 atlantic hurricane database. *Journal of Climate*, **27**, 6093 – 6118, doi:10.1175/JCLI-D-13-00503.1.

URL `https://journals.ametsoc.org/view/journals/clim/27/16/jcli-d-13-00503.1.xml`

Maloney, E. D., 2009: The moist static energy budget of a composite tropical intraseasonal oscillation in a climate model. *Journal of Climate*, **22**, 711 – 729, doi:10.1175/2008JCLI2542.1.

Mayta, V. C. and Á. F. Adames, 2023: Moist Thermodynamics of Convectively Coupled Waves over the Western Hemisphere. *Journal of Climate*, 1–34, doi:10.1175/JCLI-D-22-0435.1.

Mayta, V. C., Á. F. Adames, and F. Ahmed, 2022: Westward-propagating Moisture Mode over the Tropical Western Hemisphere. *Geophysical Research Letters*, e2022GL097799.

Mayta, V. C. and Á. F. Adames Corraliza, 2023: The Stirring Tropics. Part I: The Ubiquity of Moisture Modes and Moisture-Vortex Instability. *Journal of Climate*.

Norquist, D. C., E. E. Recker, and R. J. Reed, 1977: The energetics of african wave disturbances as observed during phase iii of gate. *Monthly Weather Review*, **105**, 334 – 342, doi:https://doi.org/10.1175/1520-0493(1977)105¡0334:TEOAWD¿2.0.CO;2.

Núñez Ocasio, K. M., A. Brammer, J. L. Evans, G. S. Young, and Z. L. Moon, 2021: Favorable monsoon environment over eastern africa for subsequent tropical cyclogenesis of african easterly waves. *Journal of the Atmospheric Sciences*, **78**, 2911 – 2925, doi:10.1175/JAS-D-20-0339.1.

URL https://journals.ametsoc.org/view/journals/atsc/78/9/JAS-D-20-0339.1.xml

Núñez Ocasio, K. M., J. L. Evans, and G. S. Young, 2020: A wave-relative framework analysis of aew–mcs interactions leading to tropical cyclogenesis. *Monthly Weather Review*, **148**, 4657 – 4671, doi:https://doi.org/10.1175/MWR-D-20-0152.1.

Núñez Ocasio, K. M. and R. Rios-Berrios, 2023: African easterly wave evolution and tropical cyclogenesis in a pre-helene (2006) hindcast using the model for prediction across scales-atmosphere (mpas-a). *Journal of Advances in Modeling Earth Systems*, **15**, e2022MS003181, doi:https://doi.org/10.1029/2022MS003181.

Pytharoulis, I. and C. Thorncroft, 1999: The Low-Level Structure of African Easterly Waves in 1995. *Monthly Weather Review*, **127**, 2266–2280, doi:10.1175/1520-0493(1999)127¡2266:TLLSOA¿2.0.CO;2.

Ruppert, J. H., A. A. Wing, X. Tang, and E. L. Duran, 2020: The critical role of cloud–infrared radiation feedback in tropical cyclone development. *Proceedings of the National Academy of Sciences*, **117**, 27884–27892, doi:10.1073/pnas.2013584117.

Russell, J. O. and A. Aiyyer, 2020: The potential vorticity structure and dynamics of african easterly waves. *Journal of the Atmospheric Sciences*, **77**, 871–890.

Russell, J. O., A. Aiyyer, and J. Dylan White, 2020: African easterly wave dynamics in convection-permitting simulations: Rotational stratiform instability as a conceptual model. *Journal of Advances in Modeling Earth Systems*, **12**, e2019MS001706.

Semunegus, H., A. Mekonnen, and C. J. Schreck III, 2017: Characterization of convective systems and their association with african easterly waves. *International Journal of Climatology*, **37**, 4486–4492, doi:https://doi.org/10.1002/joc.5085.

Thorncroft, C. D., N. M. J. Hall, and G. N. Kiladis, 2008: Three-dimensional structure and dynamics of african easterly waves. part iii: Genesis. *Journal of the Atmospheric*

Sciences, **65**, 3596–3607, doi:10.1175/2008JAS2575.1.

URL http://dx.doi.org/10.1175/2008JAS2575.1

Tomassini, L., D. J. Parker, A. Stirling, C. Bain, C. Senior, and S. Milton, 2017: The interaction between moist diabatic processes and the atmospheric circulation in african easterly wave propagation. *Quarterly Journal of the Royal Meteorological Society*, **143**, 3207–3227, doi:https://doi.org/10.1002/qj.3173.

Wing, A. A., 2022: Acceleration of tropical cyclone development by cloud-radiative feedbacks. *Journal of the Atmospheric Sciences*, **79**, 2285–2305.

Wing, A. A., S. J. Camargo, and A. H. Sobel, 2016: Role of radiative–convective feedbacks in spontaneous tropical cyclogenesis in idealized numerical simulations. *Journal of the Atmospheric Sciences*, **73**, 2633–2642.

Wing, A. A., S. J. Camargo, A. H. Sobel, D. Kim, Y. Moon, H. Murakami, K. A. Reed, G. A. Vecchi, M. F. Wehner, C. Zarzycki, and M. Zhao, 2019a: Moist Static Energy Budget Analysis of Tropical Cyclone Intensification in High-Resolution Climate Models. *Journal of Climate*, **32**, 6071 – 6095, doi:https://doi.org/10.1175/JCLI-D-18-0599.1.

Wing, A. A., S. J. Camargo, A. H. Sobel, D. Kim, Y. Moon, H. Murakami, K. A. Reed, G. A. Vecchi, M. F. Wehner, C. Zarzycki, et al., 2019b: Moist static energy budget analysis of tropical cyclone intensification in high-resolution climate models. *Journal of Climate*, **32**, 6071–6095.

Yanai, M., S. Esbensen, and J.-H. Chu, 1973: Determination of bulk properties of tropical cloud clusters from large-scale heat and moisture budgets. *J. Atmos. Sci*, **30**, 611–627.